Bioorganic Chemistry 110 (2021) 104820

Contents lists available at ScienceDirect

Bioorganic Chemistry

journal homepage: www.elsevier.com/locate/bioorg

Discovery of novel indolin-2-one compounds as potent inhibitors of HsClpP for cancer treatment

Rao Song [a,1], Yang Yang [a,1], Jiasheng Huang [a,1], Wenliang Qiao [c,1], Baozhu Luo [a], Yuan Ju [d,*], Tao Yang [a,b,*], Youfu Luo [a,*]

[a] State Key Laboratory of Biotherapy and Cancer Center/Collaborative Innovation Center for Biotherapy, West China Hospital, Sichuan University, Chengdu, Sichuan, China
[b] Laboratory of Human Diseases and Immunotherapy, West China Hospital, Sichuan University, Chengdu, Sichuan, China
[c] Lung Cancer Center, Laboratory of Lung Cancer, West China Hospital, Sichuan University, Chengdu, Sichuan, China
[d] Sichuan University Library, Sichuan University, Chengdu, Sichuan, China

ARTICLE INFO

Keywords:
HsClpP
Inhibitors
Anti-tumor
Mitochondria

ABSTRACT

Human caseinolytic protease proteolytic subunit (HsClpP) is a highly conserved serine protease that plays an essential role in cell homeostasis through removal of the damaged and/or misfolded proteins. Recently, due to its critical role in cancer proliferation and metastasis, HsClpP has been considered as a promising target for the cancer treatment. In this paper, through a random screening toward a library of 2086 bioactive chemicals, a novel compound **I**, 3-(3,5-dibromo-4-hydroxybenzylidene) -5-iodoindolin-2-one, was identified as a potent suppressor of HsClpP. Herein, a series of compound **I** derivatives were synthesized, and evaluated for their anti-cancer activities on a variety of cancers cells. Through the preliminary biological assay *in vitro,* including MTT assay and proteolytic activity assay, compound **I** was identified as the most potent inhibitor. Treatment with compound **I** impaired the migration of Hela cells. In addition, compound **I** disrupted the mitochondrial function, and reduced the level of the SDHB and induced the production of the ATF4. In general, compound **I** is a promising probe of HsClpP for cancer treatment, and is a good lead compound for the development of novel anti-cancer agent.

1. Introduction

The mitochondrion is a vital organelle of energy metabolism, of which the proteostasis is sustained by some proteolytic machineries [1]. One of the proteolytic mechanism employs HsClpP in the mitochondrial matrix which could remove proteins that are damaged and/or misfolded [2,3]. Besides, it is involved in the degradation and regulation of several enzymes of the electron transport chain and other cellular metabolic pathways [4]. In recent decades, HsClpP has been demonstrated to be related to tumor cell proliferation and metastasis [4,5].For example, the expression of HsClpP is upregulated in multiple cancers, such as lung, liver, acute myeloid leukemia, breast and ovary [6]. Since its crucial role in the proliferation and metastasis of specific types of cancer, HsClpP has been considered as an important anti-cancer drug target [4,7,8].

Chemical modulation of the proteolytic activity of HsClpP is a reliable therapeutic strategy to achieve cancer treatment. To date, HsClpP activity was mostly inhibited through modification of Ser153 residues located within its chamber by covalent inhibitors [5,9]. Three types of compounds, β-lactones [10], phenyl esters [11,12] and boric acids [13,14], were identified as HsClpP inhibitors (Fig. 1). β-lactones were developed originally as potential anti-bacterial agents to inhibit *Staphylococcus aureus* ClpP (*Sa*ClpP) [10]. Subsequently, the analogue **A2-32-01** showed potential activity to treat acute myeloid leukemia and was the first discovered HsClpP inhibitor [4]. Phenyl esters were developed

Abbreviations: HsClpP, Human caseinolytic protease proteolytic subunit; *Sa*ClpP, *Staphylococcus aureus* ClpP; ABPP, activity-based protein profiling; FITC-casein, fluorescein isothiocyanate-labeled casein; ROS, reactive oxygen species; ISR, integrated stress response.

* Corresponding authors at: State Key Laboratory of Biotherapy and Cancer Center/Collaborative Innovation Center for Biotherapy, and Laboratory of Human Disease and Immunotherapies, West China Hospital, Sichuan University, Chengdu 610041, China (T. Yang, Y. Luo). Sichuan University Library, Sichuan University, Chengdu 610041, China (Y. Ju).

E-mail addresses: yuan.ju@scu.edu.cn (Y. Ju), yangtao@wchscu.cn (T. Yang), luo_youfu@scu.edu.cn (Y. Luo).

[1] Rao Song, Yang Yang, Jiasheng Huang and Wenliang Qiao contributed equally to this work.

https://doi.org/10.1016/j.bioorg.2021.104820
Received 12 December 2020; Received in revised form 18 February 2021; Accepted 6 March 2021
Available online 10 March 2021

with improved activity and chemical stability over β-lactones. **AV-167**, a representative compound of phenyl eaters, was screened from a library of bacterial ClpP inhibitors, which also had inhibitory activity against HsClpP [12]. Gel-free quantitative activity-based protein profiling (ABPP) indicated the low selectivity of phenyl esters to many other proteins [11]. Moreover, Tan et al. identified a series of α-amino boronic acids that covalently inhibited the HsClpXP complex through a virtual screening platform [13]. Although, these aforementioned compounds exerted inhibition activity against HsClpP, several drawbacks, such as instability, poor effect, low selectivity and poor druggability, have impeded their development.

Thus, in this work, aiming to discover novel HsClpP inhibitors as anti-cancer agents, we screened an active compound library through the peptidase activity assay, and identified the compound **I** as a potential inhibitor of HsClpP. Based on the compound **I**, a series of analogues were synthesized, of which the inhibitory activity toward HsClpP and the anti-cancer activity *in vitro* were also investigated. Through the structure-activity relationship study, it was demonstrated that hydroxyl group on phenyl ring and hydrogen atom at N-1 position of indolin-2-one was crucial to the inhibitory activity. The biological activity, such as the inhibition of cell migration and the impact on mitochondrial function, and the binding mode of compound **I** with HsClpP have also been studied.

2. Results and discussion

2.1. Identification of the compound I as an HsClpP inhibitor

To discover hit compounds targeting HsClpP, we performed a random screening toward an in-house library of 2086 bioactive chemicals (Fig. 2). In the primary screening, compounds were assayed at a single-point concentration of 10 μM, and ten initial hits (hit rate 0.48%) were selected for their good inhibitory activity on HsClpP cleavage toward the substrate of AC-WLA-AMC (Fig. 3A). Then, in the secondary screening, six of ten hits have been identified with IC_{50} values below 5 μM (Fig. 3B). The proteolytic activity of HsClpP can also be determined *in vitro* by monitoring the degradation of fluorescein isothiocyanate-labeled casein (FITC-casein) substrate [15]. Using this assay, the initial hits were tested for the inhibition of proteolytic activity at concentration of 100 μM (Fig. 3C). Compound **I**, 3-(3,5-dibromo -4-hydroxybenzylidene)-5-iodoindolin-2-one, exhibited the most potential inhibitory activity toward HsClpP with IC_{50} value of 1.23 ± 0.11 μM on peptidase activity assay (substrate: AC-WLA-AMC).

2.2. Chemistry

As shown in Scheme 1, compound **I** and its 33 analogues were synthesized through the aldol reaction of aromatic aldehyde with substituted indolin-2-one building blocks in the presence of piperidine. To make clear the importance of the hydroxyl group on the aromatic ring and the hydrogen atom at N-1 position of the indolin-2-one scaffold, compounds **D13a** and **E14** were synthesized. As shown in Scheme 2, the hydroxyl group of 3,5-dibromo-4-hydroxybenzaldehyde was methylated with methyl iodide to yield intermediate **13a**, which was then reacted with the 5-nitroindolin-2-one building block to afford compound **D13a**. Compound **E14** was obtained through the aldol reaction of 2-chloro-4-hydroxybenzaldehyde (**14**) with intermediate **E** that was synthesized by methylation of indolin-2-one (**C**).

The *Z/E* configuration of some pivotal compounds were determined by 2D NOESY NMR spectrum (Table 2 and Supporting Information). The portion of Z/E configuration was judged by the co-signal of olefinic hydrogen with hydrogen at C-4 position of indolin-2-one. For instance, we found that the major peaks of the olefinic hydrogen and hydrogen at C-4 position of indolin-2-one have a co-signal in 2D NOESY NMR spectrum of compound **C13,** indicating **(*Z*)-C13** accounted for more (Fig. 4).

2.3. Inhibition of HsClpP activity in vitro

The synthesized compounds were initially evaluated for their inhibition activity against HsClpP in a fluorescence-based AC-WLA-AMC assay in independent triplicates (Table 1). Peptidase activity of HsClpP after treatment with synthesized compounds was measured by monitoring release of fluorescent amino-methylcoumarin from AC-WLA-AMC [16]. We started our investigation with modifying the indolin-2-one with different substituents. As shown in Table 1, compounds **A13**, **B13**, **C13** and **D13** showed good inhibitory activity to HsClpP with IC_{50} values of 0.79 ± 0.06, 0.76 ± 0.09, 1.69 ± 0.23 and 3.60 ± 0.49 μM, respectively. These results implied that the phenyl ring of indolin-2-one can tolerate a relative wide range of chemical space, such as hydrogen, trifluoromethyl, bromine and nitro. Besides, **E14,** obtained by methylation at N-1 position of indolin-2-one, showed decreased inhibitory activity, which indicated that the hydrogen atom of nitrogen in N-1 position was essential for the inhibitory activity. After the exploration the SAR of phenyl ring of the indolin-2-one, the SAR of C-3 position of the indolin-2-one was investigated. Among all the synthesized compounds, **A10**, **A13**, **A14**, **B10**, **B13**, **C1**, **C13**, **D1**, **D13** and **D14** with similar aromatic moieties containing hydrogen-bond donor have moderate to good inhibitory activity with IC_{50} values below 10 μM. Thus, substituents with hydrogen-bond donor were considered to be beneficial to the inhibitory activity against HsClpP. However, **C5** and **D5** bearing hydroxy on the 3′- position of phenyl group had significantly decreased inhibitory activities with IC_{50} values greater than 10 μM, which implied that hydrogen-bond donor substituted at 4′- position or 2′-position of the phenyl group is critical. Otherwise, since the inhibitory activity of **A9**, **B9** and **D16** towards HsClpP with hydrogen-bond donor was reduced, the phenyl ring substituted at C-3 position of indolin-2-one was important over 1*H*-pyrrole. To further confirm whether the hydrogen-bond donor on the phenyl ring is beneficial for the inhibitory activity, the compound **D13a** was obtained by methylation of hydroxyl group of **D13**. Compound **D13a** exhibited weak activity against HsClpP, indicating that the hydroxyl group of the phenyl ring is the key element of these HsClpP inhibitors.

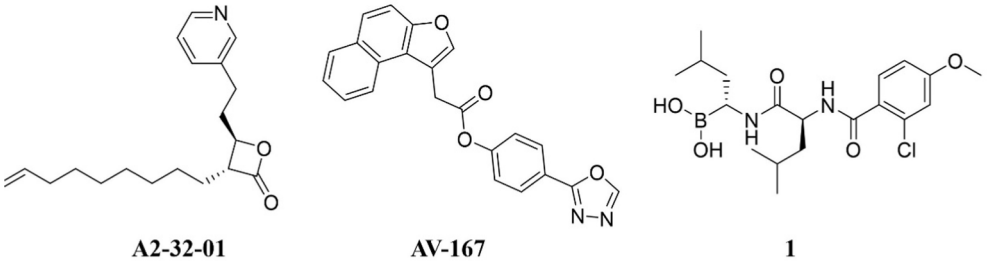

Fig. 1. Representative inhibitors against HsClpP.

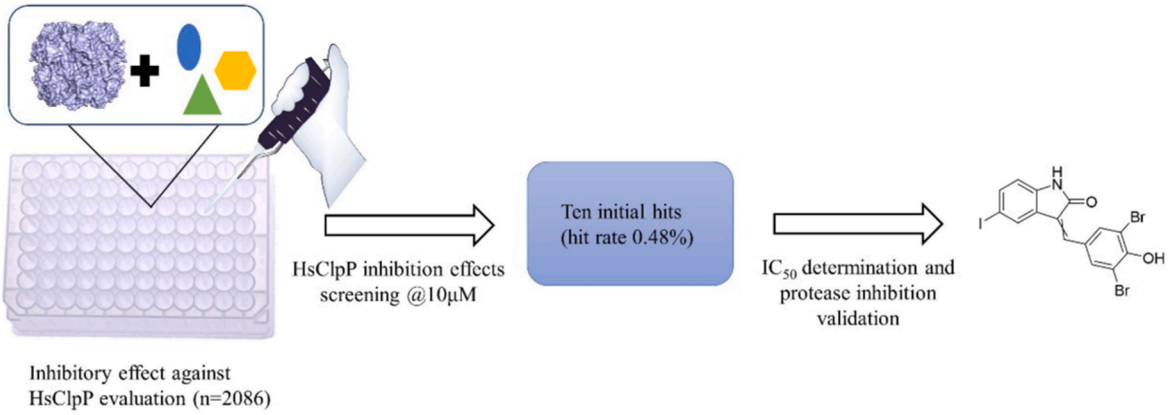

Fig. 2. Schematic illustration of chemical screening. Identification of novel HsClpP inhibitor hits in an in-house library of 2086 bioactive chemicals.

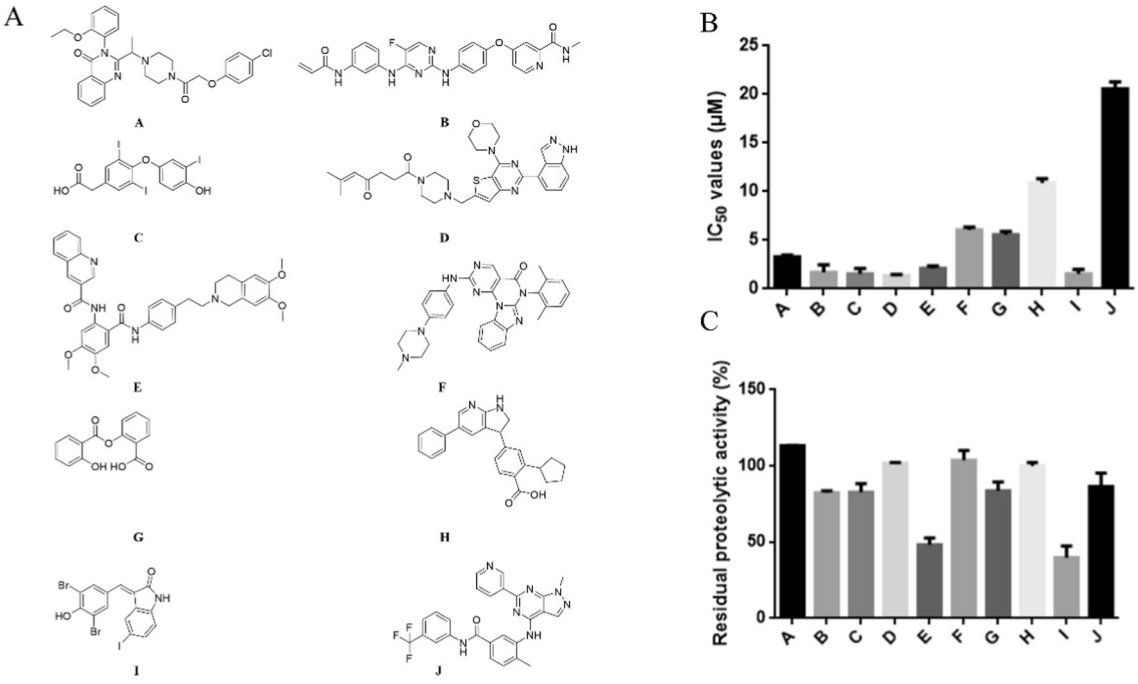

Fig. 3. Discovery of a novel HsClpP inhibitor from a bioactive chemical library screening. (**A**) A random screening of 2086 compounds identified ten primary hits with good inhibitory effect at 10 μM. (**B**) IC_{50} values of compounds **A-J** toward HsClpP. (**C**) Inhibition of HsClpP proteolytic activity by 100 μM compounds **A-J** in the FITC-casein substrate.

2.4. Inhibition of HsClpP induces anti-tumor effects in vitro.

The expression of HsClpP is upregulated in multiple cancer cells, which is essential for the proliferation of cancer cells. To evaluate the anticancer activities of synthesized compounds, four human cancer cell lines (HepG2, Hela, HCT116 and Skov3) were treated with these compounds (Table 3). Compounds with IC_{50} values below 10 μM in peptidase activity assay were assessed for their anti-proliferation activity using MTT assay. As shown in Table 2, compound **I** showed good inhibitory activities against HepG2, Hela, HCT116 and Skov3 cells with IC_{50} values of 14.42 ± 0.93, 11.81 ± 1.24, 18.99 ± 0.29, 37.47 ± 3.03 μM, respectively. While the control **AV167**, exhibited almost no inhibition activity against all four cell lines at the concentration of 40 μM. The inhibition activity of **A10**, **B10**, **C1** and **D1** significantly decreased, compared with that of compound **I**. Compound **B13**, with trifluoromethyl group substituted at the indolin-2-one ring, and **C13** inhibited the growth of HepG2, Hela, HCT116 and Skov3 cells with IC_{50} values comparable to that of compound **I**. Moreover, the synthesized compounds showed almost no inhibition activity on HsClpP-negative MCF-7 cells at the concentration of 40 μM, which demonstrated a good selectivity on HsClpP highly expression cell lines.

To assess the ability of blocking proteolytic activity of selected compounds, HsClpP was activated via the ONC201 derived chaperone mimic for inducing pore opening and digesting of FITC-casein [16]. (Fig. 4A). Using this assay, AV167 and the selected compounds towards the inhibitory proteolytic activity of HsClpP were assessed at three concentrations of 100 μM, 10 μM and 1 μM in independent triplicates (Fig. 5A). Similarly to **AV167**, compounds **I**, **A13** and **B13** showed good inhibition activity at the highest concentration, which demonstrated that compounds **I**, **A13** and **B13** could efficiently block proteolysis through inhibition of HsClpP.

Previous investigation indicated that an increase of the expression of HsClpP is crucial for proliferation and metastasis of certain cancer cell lines, and *CLPP* knockdown in cancer cells resulted in inhibition of cell migration [4]. In this work, migration of Hela cells was impaired after incubation with compound **I** for 24 h (Fig. 5B).

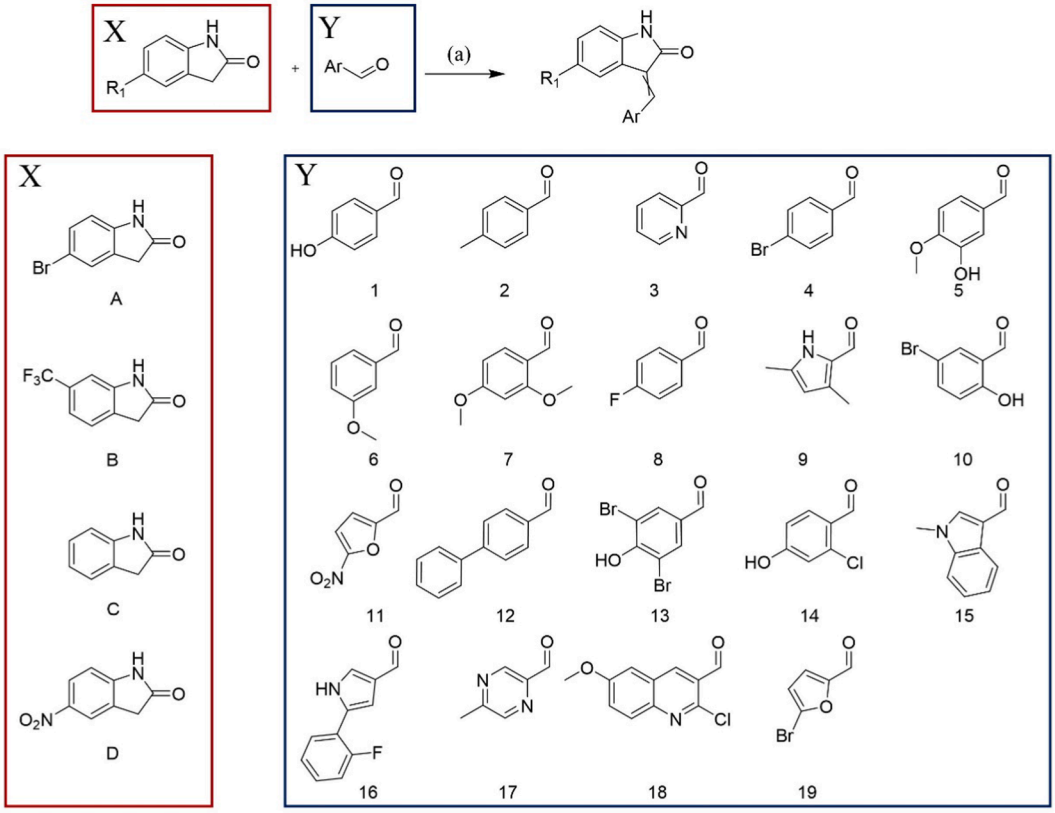

Scheme 1. Synthetic strategy of target compounds. Reagents and conditions: (a) piperidine, MeOH, 65 °C.

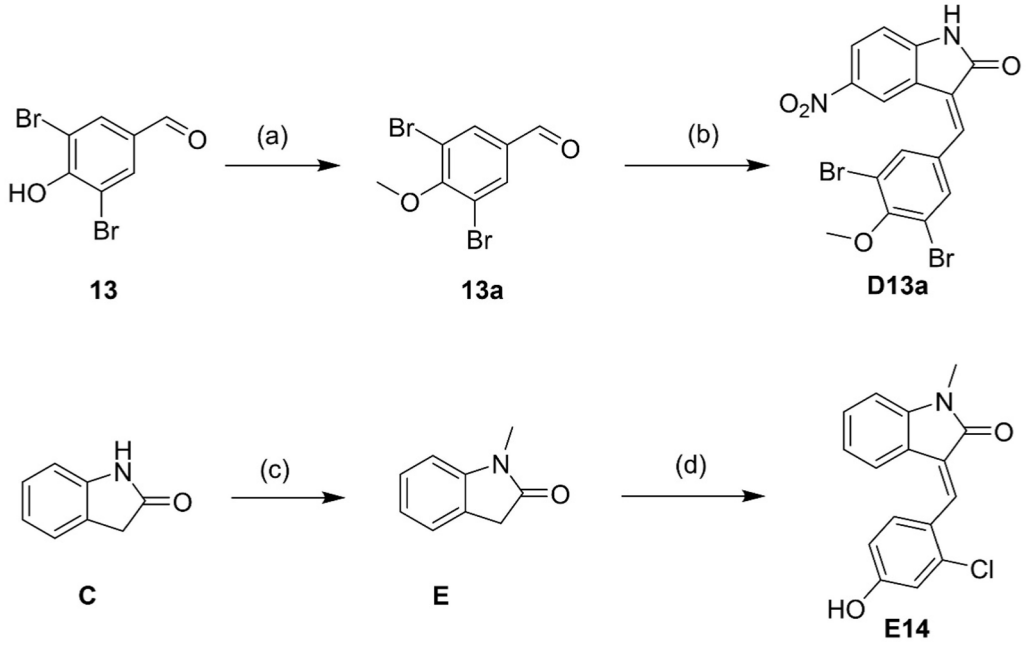

Scheme 2. Synthesis of compounds **D13a** and **E14**. Reagents and conditions: (a) K_2CO_3, CH_3I, DMF, rt. (b) 5-nitroindolin-2-one, piperidine, MeOH, 65 °C. (c) $(CH_3)_2SO_4$, PhMe, 100 °C. (d) 2-chloro-4-hydroxybenzaldehyde, piperidine, MeOH, 65 °C.

2.5. The binding mode of compound I with HsClpP

To explore the possible interaction modes of the selected compounds with HsClpP, substrate competition assay was performed in the presence of 200 μM, 100 μM or 50 μM AC-WLA-AMC substrate in independent triplicates (Fig. 6A). With the concentration of substrate increased, the IC_{50} values of **AV167** and compound **I** increased, indicative of a competitive binding with HsClpP. In order to further define the binding mode of compound **I** with HsClpP, molecular docking studies were performed with Schrodinger. The structure of the HsClpP was obtained from the Protein Data Bank. We generated 3D diagrams to show the binding mode of compound **I** within the HsClpP (Fig. 6B). Although,

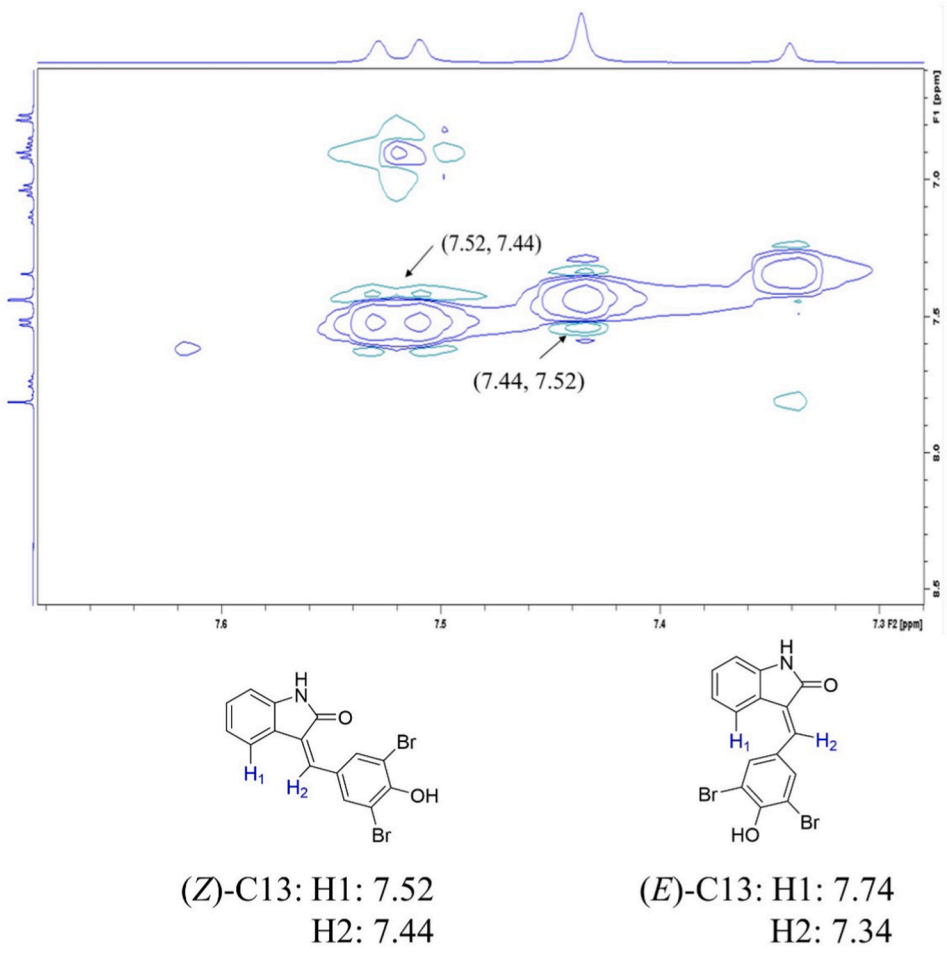

Fig. 4. The 2D NOESY NMR spectrum (part) of compound **C13**. The portion of *Z/E* configuration was judging from the existing of co-signal of olefinic hydrogen with hydrogen at C-4 position.

compound **I** did not directly bound to catalytic Ser97 residue, it is tightly bound to residues surrounding the active site such as Pro66 and Gln138. As shown in Fig. 5B, compound **I** binds to the HsClpP by hydrogen bonds of Pro66 and Gln138 with NH and hydroxy, which is consistent with the peptidase activity assay of **D13a** and **E14**.

*2.6. HsClpP inhibition by compound **I** and **B13** leads to the mitochondria impaired and induction of integrated stress response*

We then studied the effects of HsClpP inhibition on mitochondrial function. In cancer cells, the elevation of reactive oxygen species (ROS) in mitochondria is important for facilitating and sustaining oncogenesis. Inhibition of HsClpP increased the production of mitochondrial ROS that will induce cell apoptosis [4]. Treatment with compound **I** and **B13** increased the production of mitochondrial ROS in Hela cells, which is 4.4-fold and 3.3-fold over the control group at the concentration of 10 μM for 48 h, respectively. (Fig. 7A). Respiratory chain subunit SDHB had previously been considered as putative HsClpP substrates, and the inhibition of HsClpP may reduce the enzymatic activity of SDHB [4,5]. In addition, influence of the function of HsClpP could induce an integrated stress response (ISR) by the induction of ATF4 [5,15]. Further, we treated Hela cells with compound **I** and **B13** and found that both the compound **I** and **B13** reduced the level of the SDHB and induced the production of ATF4 in a dose-dependent manner (Fig. 7B).

3. Conclusion

In summary, a novel compound **I**, (3-(3,5-dibromo-4-hydroxybenzylidene)- -5-iodoindolin-2-one), was identified as HsClpP inhibitor. Based on the compound **I**, a series of analogues have been synthesized, some of which exerted promising inhibition activity on peptidase and protease assay of HsClpP. Besides, they exhibited potent anti-proliferation activity on HepG2, Hela, HCT116 and Skov3 cell lines, while no obvious activity to HsClpP-negative MCF-7 cells. In addition to the anti-proliferation activity, compound **I** inhibited the migration of Hela cells. Also, treatment with compound **I** reduced the level of the SDHB and induced the production of ATF4 in a dose-dependent manner to impair the oxidative phosphorylation. Generally, compound **I** is worth of further investigation toward the discovery of HsClpP inhibitor as a valuable lead compound for oncotherapy.

4. Experimental section

4.1. Chemistry

All reagents were directly used as purchased without further purification. All solvents were dried according to standard methods before use, solvents used in optical spectroscopic studies were HPLC grade. All NMR spectrum were recorded on a Bruker Avance (Varian Unity Inova) 500 MHz spectrometer in DMSO-d_6 with tetramethylsilane (TMS) as internal standard. ^{1}H NMR and ^{13}C NMR spectra were recorded respectively at 400 MHz and 100 MHz. ^{1}H NMR and ^{13}C NMR were analyzed by MestReNova Software. High resolution mass spectrum (HRMS) was performed on an Agilent LC/MSD TOF system G3250AA. Analytical thin layer chromatography (TLC) was performed on silica gel 60 F254 precoated plates (0.25 mm) from Qingdao Haiyang Inc., and

Table 1
The inhibition activity of target compounds toward HsClpP in the AC-WLA-AMC assay.

Compd.	I	II	IC_{50}(μM)	Compd.	I	II	IC_{50}(μM)
I	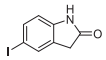		1.23 ± 0.11	C11		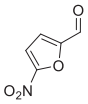	>10
A3	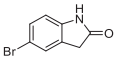		>10	C12		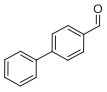	>10
A4	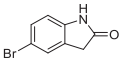		>10	C13			1.69 ± 0.23
A6	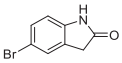	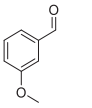	>10	C15			>10
A7	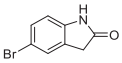	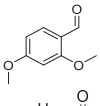	>10	C17			>10
A9	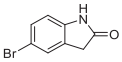	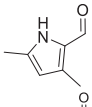	>10	C18		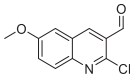	>10
A10	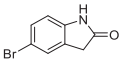	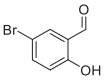	3.11 ± 0.09	C19			>10
A13	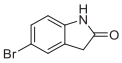		0.79 ± 0.06	D1	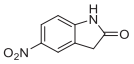		2.43 ± 0.30
A15	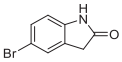		>10	D2	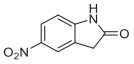		>10
B3	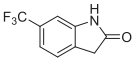		>10	D3	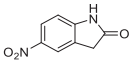		>10
B9			>10	D5			>10
B10			5.99 ± 0.30	D12			>10
B13			0.76 ± 0.09	D13			3.60 ± 0.49
C1			9.42 ± 0.97	D14			1.76 ± 0.66
C2			>10	D15			>10
C5			>10	D16			>10
C6			>10	D13a			>10
C8			>10	E14			>10

Table 2
The Z/E configuration of some key compounds.

Compd.	Structure	Configuration	Compd.	Structure	Configuration
I	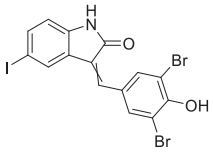	Z/E≈1/9	C1	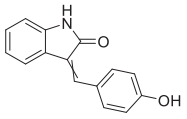	E
A10	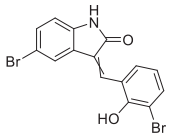	Z/E≈1/9	C13	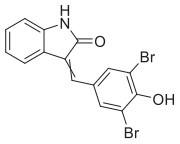	Z/E≈4/1
A13	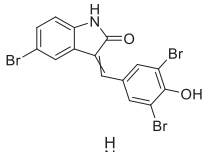	Z/E≈4/1	D1	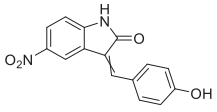	Z/E≈4/1
B10	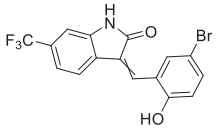	Z/E≈2/3	D13	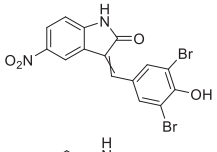	Z/E≈4/1
B13	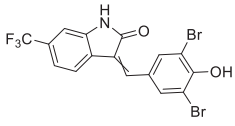	Z/E≈7/3	D14	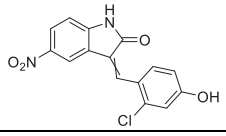	Z/E≈1/4

Table 3
Anti-proliferation activity of selected compounds against HepG2, Hela, HCT116, Skov3 and MCF-7 cells.

Compd.	IC_{50}(μM)				
	HepG2	Hela	HCT166	Skov3	MCF-7
A10	>40	>40	>40	>40	>40
A13	>40	31.35 ± 0.64	36.18 ± 3.18	>40	>40
B10	>40	>40	>40	>40	>40
B13	12.84 ± 0.65	10.66 ± 0.58	14.64 ± 1.31	27.51 ± 1.69	>40
C1	>40	>40	>40	>40	>40
C13	11.61 ± 0.94	10.34 ± 0.65	13.75 ± 0.97	28.00 ± 2.65	>40
D1	>40	>40	>40	>40	>40
D13	12.62 ± 1.36	11.25 ± 0.32	32.10 ± 0.65	>40	>40
D14	24.81 ± 1.55	16.56 ± 1.04	23.01 ± 1.87	27.99 ± 1.12	>40
I	14.42 ± 0.93	11.81 ± 1.24	18.99 ± 0.29	37.47 ± 3.03	>40
AV167	>40	>40	>40	>40	>40

components were visualized by ultraviolet light (254 nm). Silicycle silica gel 300–400 (particle size 40–63 μm) mesh was used for all flash column chromatography experiments.

4.2. General procedure for synthesis of compounds

To a solution of the corresponding starting materials (200 mg, 1 eq.) in MeOH (2 mL), piperidine (1.5 eq.) and corresponding aromatic aldehydes (1.2 eq.) were added. The reaction mixture was heated to 65 °C and stirred for 1–8 h, then cooled to room temperature. The mixture was added with water (10 mL) and extracted with DCM (10 mL) for three times, the combined organic layer was washed with brine and dried over anhydrous sodium sulfate. Then purified by column chromatography to give products.

4.2.1. 5-Bromo-3-(pyridin-2-ylmethylene)indolin-2-one (**A3**)

^{1}H NMR (400 MHz, DMSO) δ 10.76 (s, 1H), 9.28 (m, 1H), 8.89 (d, J = 4.1 Hz, 1H), 8.00 (dd, J = 7.6, 2.0 Hz, 1H), 7.92 (d, J = 8.0 Hz, 1H), 7.63 (s, 1H), 7.54–7.44 (m, 1H), 6.84 (d, J = 8.0 Hz, 1H).^{13}C NMR (101 MHz, DMSO) δ 169.33, 153.30, 150.07, 143.20, 138.00, 135.77, 133.52, 130.85, 129.58, 128.70, 125.14, 124.04, 113.36, 111.96. HRMS (Q-TOF): calculated for $C_{14}H_9BrN_2O_1$ 299.9898 $[M + H]^+$, found 300.9981. Purity ≥ 95.0%.

4.2.2. 5-Bromo-3-(4-bromobenzylidene)indolin-2-one (**A4**)

^{1}H NMR (400 MHz, DMSO) δ 10.79 (s, 1H), 7.76 (d, J = 8.4 Hz, 2H), 7.70–7.63 (m, 3H), 7.51 (d, J = 1.6 Hz, 1H), 7.42 (dd, J = 8.4, 2.0 Hz, 1H), 6.85 (d, J = 8.4 Hz, 1H). ^{13}C NMR (101 MHz, DMSO) δ 168.45, 142.68, 136.72, 133.77, 133.14, 132.33, 131.78, 127.70, 125.06, 123.86, 123.25, 113.18, 112.57. HRMS (Q-TOF): calculated for $C_{15}H_9Br_2NO$ 376.9051 $[M + Na]^+$, found 399.8946. Purity ≥ 95.0%.

4.2.3. 5-Bromo-3-(3-methoxybenzylidene)indolin-2-one (**A6**)

^{1}H NMR (400 MHz, DMSO) δ 10.74 (s, 1H), 7.71 (s, 1H), 7.65 (d, J = 7.2 Hz, 1H), 7.57–7.50 (m, 1H), 7.44–7.38 (m, 2H), 7.20 (d, J = 8.0 Hz, 1H), 7.11 (t, J = 7.2 Hz, 1H), 6.84 (d, J = 8.4 Hz, 1H), 3.87 (s, 3H).^{13}C NMR (101 MHz, DMSO) δ 168.59, 158.13, 142.32, 134.12, 132.70, 132.62, 130.05, 126.94, 125.05, 123.72, 122.86, 120.71, 113.05, 112.36, 112.21, 56.09. HRMS (Q-TOF): calculated for $C_{16}H_{12}BrNO_2$ 329.0051 $[M + H]^+$, found 330.0131. Purity ≥ 95.0%.

4.2.4. 5-Bromo-3-(2,4-dimethoxybenzylidene)indolin-2-one (**A7**)

^{1}H NMR (400 MHz, $CDCl_3$) δ 8.02 (s, 1/4H), 7.99 (s, 3/4H), 7.82 (s, 3/4H), 7.76 (d, J = 2 Hz, 1H), 7.66 (m, 1H), 7.33–7.27 (m, 1H), 6.74 (m, 1H), 6.60 (m, 1H), 6.53 (d, J = 2.4 Hz, 3/4H), 6.45 (d, J = 2.4 Hz, 1/4H), 5.30 (s, 1/4H), 3.90 (m, 6H).^{13}C NMR (101 MHz, DMSO) δ 168.95, 163.62, 160.05, 141.99, 134.03, 132.09, 131.25, 124.72, 124.68, 124.07, 115.45, 112.99, 112.20, 106.00, 99.07, 56.28, 56.10. HRMS (Q-TOF): calculated for $C_{17}H_{14}BrNO_3$ 359.0157 $[M + H]^+$, found 360.0256.

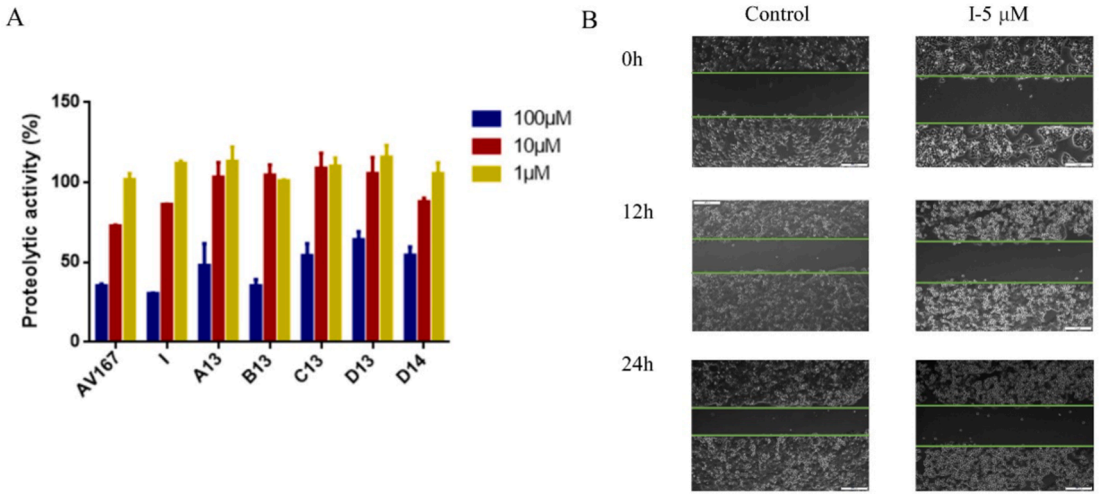

Fig. 5. (**A**) FITC-casein degradation assay with HsClpP, ONC201 and inhibitors at three different concentrations. (**B**) Scratch test in Hela cells by treatment with compound **I** at 5 μM for 24 h.

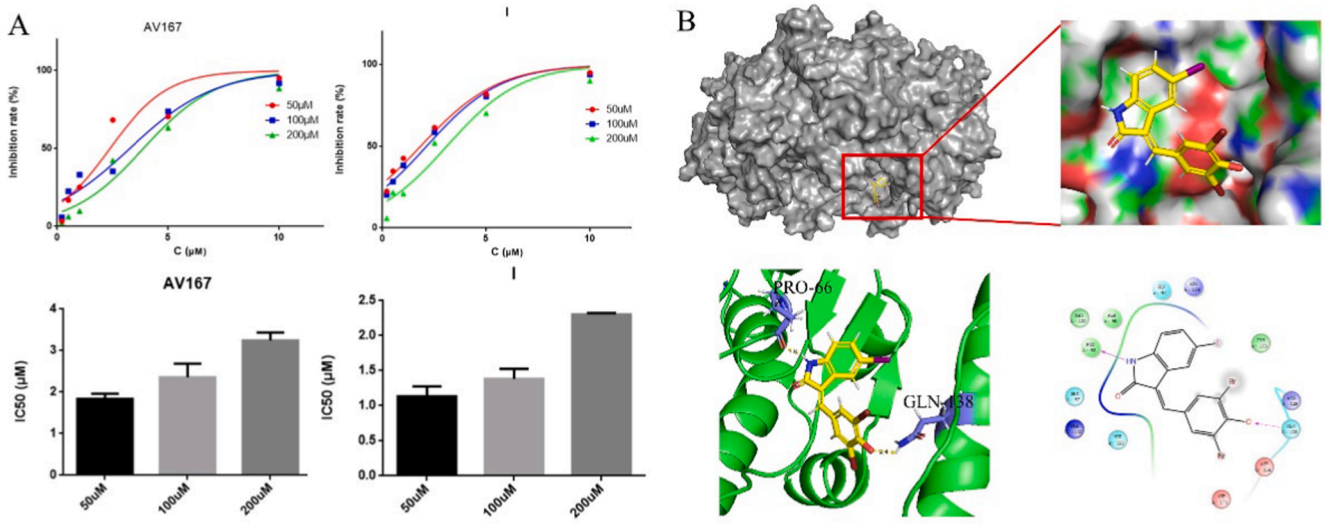

Fig. 6. The binding mode of compound **I** with HsClpP. (**A**) IC50 values of AV167 and compound **I** in the presence of 200 μM, 100 μM or 50 μM AC-WLA-AMC substrate. (**B**) 3D and 2D diagrams to show the binding mode through molecular docking study.

Purity ≥ 95.0%.

*4.2.5. 5-Bromo-3-((3,5-dimethyl-1H-pyrrol-2-yl)methylene)indolin-2-one **(A9)***

^{1}H NMR (400 MHz, DMSO) δ 13.38 (s, 1H), 10.87 (s, 1H), 8.02 (d, J = 2 Hz, 1H), 7.69 (s, 1H), 7.22 (dd, J = 8.0, 2.0 Hz, 1H), 6.81 (d, J = 8.4 Hz, 1H), 6.04 (d, J = 2.0 Hz, 1H), 2.32 (d, J = 2.4 Hz, 6H).^{13}C NMR (101 MHz, DMSO) δ 169.58, 137.37, 137.34, 133.68, 128.87, 128.04, 127.41, 125.48, 121.21, 113.62, 113.46, 111.63, 111.39, 14.03, 11.79. HRMS (Q-TOF): calculated for $C_{15}H_{13}BrN_2O$ 316.0211 $[M + H]^+$, found 317.0228. Purity ≥ 95.0%.

*4.2.6. 5-Bromo-3-(5-bromo-2-hydroxybenzylidene)indolin-2-one **(A10)***

^{1}H NMR (400 MHz, DMSO) δ 10.81–10.48 (m, 2H), 7.92 (s, 1/10*H*), 7.81 (d, J = 1.6 Hz, 1/10*H*), 7.72 (d, J = 2.4 Hz, 9/10*H*), 7.62 (s, 9/10*H*), 7.53–7.35 (m, 2H), 6.96 (d, J = 8.8 Hz, 9/10*H*), 6.89 (d, J = 8.8 Hz, 1/10*H*), 6.84 (d, J = 8.0 Hz, 9/10*H*), 6.79 (d, J = 8.0 Hz, 1/10*H*).^{13}C NMR (101 MHz, DMSO) δ 168.52, 156.24, 142.45, 134.50, 132.78, 132.72, 132.08, 127.33, 125.41, 123.68, 123.65, 118.79, 113.08, 112.42, 110.13. HRMS (Q-TOF): calculated for $C_{15}H_9Br_2N_1O_2$ 392.9000 $[M + Na]^+$, found 415.8867. Purity ≥ 95.0%.

*4.2.7. 5-Bromo-3-(3,5-dibromo-4-hydroxybenzylidene)indolin-2-one **(A13)***

^{1}H NMR (400 MHz, DMSO) δ 10.43 (s, 1/5H), 10.35 (s, 4/5H), 8.74 (s, 8/5H), 7.84 (d, J = 1.6 Hz, 1/5H), 7.79 (s, 2/5H), 7.71 (d, J = 1.6 Hz, 4/5H), 7.51 (s, 4/5H), 7.37 (s, 1/5H), 7.27 (dd, J = 8.4, 2.0 Hz, 1/5H), 7.13 (dd, J = 8.4, 2.0 Hz, 4/5H), 6.79 (d, J = 8.0 Hz, 1/5H), 6.70 (d, J = 8.0 Hz, 4/5H).^{13}C NMR (101 MHz, DMSO) δ 167.90, 139.32, 138.19, 137.74, 135.17, 130.09, 127.51, 120.33, 117.94, 115.33, 112.83, 110.65. HRMS (Q-TOF): calculated for $C_{15}H_8Br_3NO_2$ 470.8105 $[M + Na]^+$, found 493.7997. Purity ≥ 95.0%.

*4.2.8. 5-Bromo-3-((1-methyl-1H-indol-3-yl)methylene)indolin-2-one **(A15)***

^{1}H NMR (400 MHz, DMSO) δ 10.65 (s, 1H), 9.43 (s, 1H), 8.31 (m, 1H), 8.26 (s, 1H), 8.19 (d, J = 1.6 Hz, 1H), 7.59 (d, J = 7.6 Hz, 1H), 7.30 (m,3H), 6.79 (d, J = 8.4 Hz, 1H), 3.95 (s, 3H). ^{13}C NMR (101 MHz, DMSO) δ 168.18, 138.50, 138.08, 137.06, 129.33, 129.21, 129.17, 128.57, 123.24, 121.95, 121.70, 119.40, 118.01, 113.27, 111.23, 111.18, 111.08, 34.02. HRMS (Q-TOF): calculated for $C_{18}H_{13}BrN_2O$ 352.0211 $[M + H]^+$, found 353.0319.Purity ≥ 95.0%.

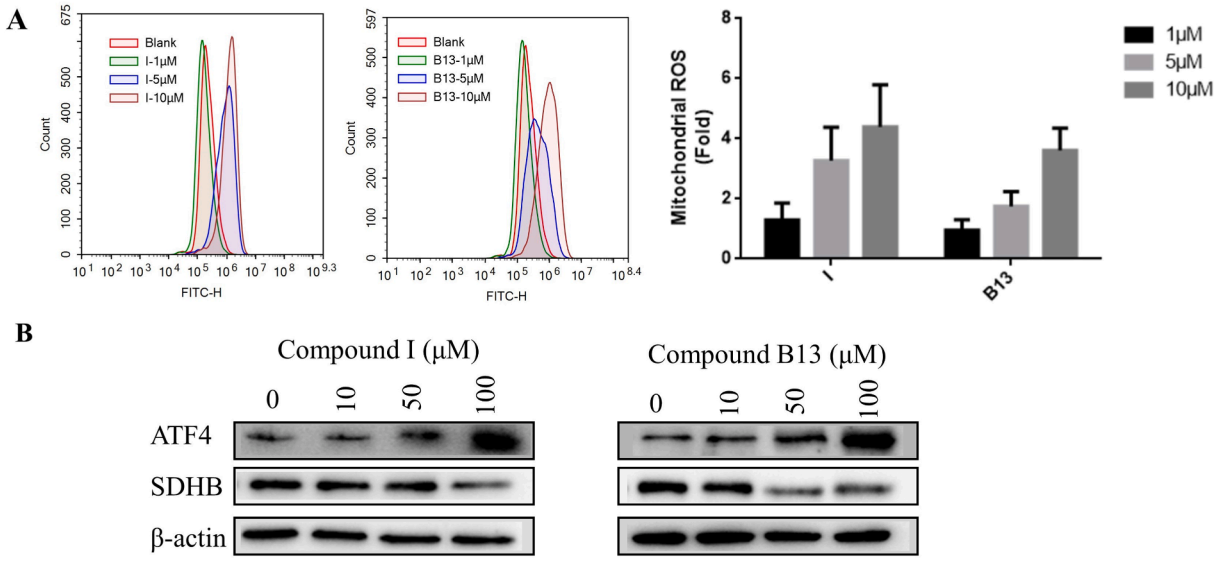

Fig. 7. HsClpP inhibition by compound **I** and **B13** impairs oxidative phosphorylation. (**A**) Effect of compound **I** and **B13** treatment on mitochondrial reactive oxygen species (ROS) production in Hela cells for 48 h. (**B**) Western blot of ATF4 and SDHB in Hela cells with compound **I** and **B13**-inducible for 24 h at the indicated concentrations.

*4.2.9. 3-(Pyridin-2-ylmethylene)-6-(trifluoromethyl)indolin-2-one (**B3**)*

^{1}H NMR (400 MHz, DMSO) δ 10.99 (s, 1/2H), 10.91 (s, 1/2H), 9.26 (d, J = 8.0 Hz, 1/2H), 8.94 (m, 1H), 8.73 (d, J = 4.0 Hz, 1/2H), 8.06–7.87 (m, 2.5H), 7.74 (s, 1/2H), 7.57–7.50 (m, 1/2H), 7.44 (m, 1/2H), 7.36 (d, J = 8.0 Hz, 1H), 7.08 (d, J = 12.0 Hz, 1H).^{13}C NMR (101 MHz, DMSO) δ 169.42, 153.11, 150.23, 144.48, 137.91, 137.27, 130.62 (q, J = 31.7 Hz), 129.65, 128.95, 128.31, 125.74, 125.63, 125.24, 118.43 (q, J = 4.0 Hz), 106.11 (q, J = 3.9 Hz). HRMS (Q-TOF): calculated for $C_{15}H_9Br_3N_2O$ 290.0667 $[M + H]^+$, found 291.0740. Purity $\geq$ 95.0%.

*4.2.10. 3-((3,5-Dimethyl-1H-pyrrol-2-yl)methylene)-5-(trifluoromethyl) indolin-2-one (**B9**)*

^{1}H NMR (400 MHz, DMSO) δ 13.44 (s, 1H), 11.03 (s, 1H), 7.94 (d, J = 7.6 Hz, 1H), 7.75 (s, 1H), 7.31 (d, J = 8.0 Hz, 1H), 7.09 (s, 1H), 6.09 (d, J = 2.0 Hz, 1H), 2.34 (d, J = 4.8 Hz, 6H). ^{13}C NMR (101 MHz, DMSO) δ 169.78, 138.40, 138.26, 134.59, 130.49, 127.60, 126.58, 126.18, 125.60 (d, J = 31.3 Hz), 118.65, 118.00, 113.88, 111.00, 105.83, 14.07, 11.81. HRMS (Q-TOF): calculated for $C_{16}H_{13}F_3N_2O$ 306.0980 $[M + H]^+$, found 307.1051. Purity $\geq$ 95.0%.

*4.2.11. 3-(5-Bromo-2-hydroxybenzylidene)-6-(trifluoromethyl)indolin-2-one (**B10**)*

^{1}H NMR (400 MHz, DMSO) δ 10.85 (s, 1H), 8.97 (d, J = 2.4 Hz, 2/5H), 8.10 (s, 2/5H), 7.79–7.71 (m, 8/5H), 7.53 (d, J = 8.0 Hz, 3/5H), 7.48 (dd, J = 8.8, 2.4 Hz, 3/5H), 7.38 (d, J = 9.6 Hz, 2/5H), 7.29 (m, 1H), 7.09 (s, 3/5H), 7.03 (s, 2/5H), 6.93 (d, J = 8.8 Hz, 3/5H), 6.79 (s, 2/5H). 13C NMR (101 MHz, DMSO) δ 190.06, 168.65, 167.35, 160.37, 157.29, 156.34, 143.74, 141.53, 138.89, 135.64, 134.72, 134.30, 133.11, 132.06, 130.86, 130.03 (d, J = 31.9 Hz), 126.99, 125.79, 125.32, 124.48, 123.66, 123.29, 122.93 (d, J = 31.8 Hz), 120.64, 120.38, 118.79, 118.49, 118.08, 111.15, 110.31, 110.07, 106.61. HRMS (Q-TOF): calculated for C16H9BrF3NO2 382.9769 [M + H]+, found 384.3070. Purity $\geq$ 95.0%.

*4.2.12. 3-(3,5-Dibromo-4-hydroxybenzylidene)-6-(trifluoromethyl) indolin-2-one (**B13**)*

^{1}H NMR (400 MHz, DMSO) δ ^{1}H NMR (400 MHz, DMSO) δ 10.99 (s, 7/10*H*), 10.95 (s, 3/10*H*), 8.84 (s, 7/5H), 7.95 (s, 3/5H), 7.92 (s, 7/10*H*), 7.86 (d, J = 8.0 Hz, 7/10*H*), 7.66 (m, 3/5H), 7.37 (d, J = 8.0 Hz, 7/10*H*), 7.28 (d, J = 8.0 Hz, 3/10*H*), 7.12 (s, 3/10*H*), 7.07 (s, 7/10*H*).13C NMR (101 MHz, DMSO) δ 168.58, 167.45, 153.70, 152.90, 143.92, 141.27, 137.74, 137.10, 136.95, 134.12, 133.91, 130.99, 129.31, 129.13, 128.82, 128.71, 128.60, 126.74, 126.09, 124.93, 123.38, 122.87, 120.56, 118.46, 112.48, 112.33, 111.56, 106.03. HRMS (Q-TOF): calculated for $C_{16}H_8Br_2F_3NO_2$ 462.8851 $[M + H]^+$, found 463.2195. Purity $\geq$ 95.0%.

*4.2.13. 3-(4-Hydroxybenzylidene)indolin-2-one (**C1**)*

^{1}H NMR (400 MHz, DMSO) δ 10.50 (s, 1H), 10.11 (s, 1H), 7.69 (d, J = 7.6 Hz, 1H), 7.62 (d, J = 8.4 Hz, 2H), 7.54 (s, 1H), 7.21 (td, J = 7.6, 0.8 Hz, 1H), 6.96–6.84 (m, 4H).^{13}C NMR (101 MHz, DMSO) δ 169.52, 159.74, 142.96, 137.05, 132.28, 129.87, 125.49, 125.14, 122.51, 121.79, 121.47, 116.11, 110.40. HRMS (Q-TOF): calculated for $C_{15}H_{11}NO_2$ 237.0790 $[M + H]^+$, found 238.0869. Purity $\geq$ 95.0%.

*4.2.14. 3-(4-Methylbenzylidene)indolin-2-one (**C2**)*

^{1}H NMR (400 MHz, DMSO) δ 10.57 (s, 1H), 8.32 (d, J = 8.4 Hz, 1/10*H*), 7.76 (s, 1/10*H*), 7.71–7.55 (m, 19/5H), 7.34 (d, J = 8.0 Hz, 9/5H), 7.28 (d, J = 8.4 Hz, 1/10*H*), 7.22 (m, 1H), 6.98 (td, J = 7.6 ,0.8 Hz, 1/10*H*), 6.92–6.80 (m, 2H), 2.38 (m, 3H). ^{13}C NMR (101 MHz, DMSO) δ 169.20, 143.32, 140.15, 136.43, 132.03, 130.44, 129.88, 129.81, 127.42, 122.74, 121.54, 121.49, 110.56, 21.57. HRMS (Q-TOF): calculated for $C_{16}H_{13}NO_2$ 235.0997 $[M + H]^+$, found 236.1059. Purity $\geq$ 95.0%.

*4.2.15. 3-(3-Hydroxy-4-methoxybenzylidene)indolin-2-one (**C5**)*

^{1}H NMR (400 MHz, DMSO) δ 10.52 (s, 1H), 9.37 (s, 7/10*H*), 8.17 (d, J = 2.0 Hz,3/10*H*), 7.83 (dd, J = 8.4, 2.0 Hz, 3/10*H*), 7.73 (d, J = 7.6 Hz, 7/10*H*), 7.69–7.63 (m, 3/5H), 7.49 (s, 7/10*H*), 7.26–7.13 (m, 27/10*H*), 7.04 (m, 1H), 6.96 (m, 3/10*H*), 6.92–6.83 (m, 14/10*H*), 6.80 (d, J = 7.6 Hz, 3/10*H*), 3.85 (s, 3H). ^{13}C NMR (101 MHz, DMSO) δ 168.71, 144.81, 142.35, 138.79, 137.17, 131.27, 129.20, 126.85, 123.43, 121.98, 119.60, 116.61, 114.94, 111.34, 109.25, 33.99. HRMS (Q-TOF): calculated for $C_{16}H_{13}NO_3$ 267.0895 $[M + H]^+$, found 268.0975. Purity $\geq$ 95.0%.

*4.2.16. 3-(3-Methoxybenzylidene)indolin-2-one (**C6**)*

^{1}H NMR (400 MHz, DMSO) δ 10.59 (s, 1H), 7.60 (s, 1H), 7.55 (d, J = 7.6 Hz, 1H), 7.45 (t, J = 8.0 Hz, 1H), 7.30–7.20 (m, 3H), 7.05 (dd, J = 8.4, 2.4 Hz, 1H), 6.87 (m, 2H), 3.81 (s, 3H). ^{13}C NMR (101 MHz, DMSO) δ 169.10, 158.10, 143.22, 132.22, 132.19, 130.37, 129.98, 127.79,

123.30, 122.73, 121.56, 121.50, 120.67, 112.00, 110.51, 56.03. HRMS (Q-TOF): calculated for $C_{16}H_{13}NO_2$ 251.0946 $[M + H]^+$, found 252.1028. Purity ≥ 95.0%.

*4.2.17. 3-(4-Fluorobenzylidene)indolin-2-one (**C8**)*

^{1}H NMR (400 MHz, DMSO) δ 10.60 (s, 1H), 7.78 (m, 2H), 7.61 (s, 1H), 7.50 (d, *J* = 7.6 Hz, 1H), 7.36 (t, *J* = 8.8 Hz, 2H), 7.24 (t, *J* = 7.6 Hz, 1H), 6.93–6.81 (m, 2H). ^{13}C NMR (101 MHz, DMSO) δ 169.03, 163.02 (d, *J* = 249.1 Hz), 143.47, 135.15, 132.26, 132.17, 131.37 (d, *J* = 249.1 Hz), 130.68, 128.10, 122.77, 121.63, 121.23, 116.42, 116.20, 110.65. HRMS (Q-TOF): calculated for $C_{15}H_{10}FNO$ 239.0746 $[M + H]^+$, found 240.0622. Purity ≥ 95.0%.

*4.2.18. 3-((5-Nitrofuran-2-yl)methylene)indolin-2-one (**C11**)*

^{1}H NMR (400 MHz, DMSO) δ 10.91 (s, 1H), 8.19 (s, 1H), 8.16 (d, *J* = 4.4 Hz, 1H), 7.77 (d, *J* = 4.8 Hz, 1H), 7.74 (d, *J* = 8.4 Hz, 1H), 7.30 (td, *J* = 7.6, 0.8 Hz, 1H), 7.05 (td, *J* = 7.6, 0.8 Hz, 1H), 6.90 (d, *J* = 7.6 Hz, 1H). ^{13}C NMR (101 MHz, DMSO) δ 167.76, 153.67, 143.46, 142.09, 136.55, 130.90, 129.22, 127.59, 127.10, 123.77, 122.00, 121.14, 110.54. HRMS (Q-TOF): calculated for $C_{13}H_8N_2O_4$ 256.0484 $[M + H]^+$, found 256.0964. Purity ≥ 95.0%.

*4.2.19. 3-([1,1′-Biphenyl]-4-ylmethylene)indolin-2-one (**C12**)*

^{1}H NMR (400 MHz, DMSO) δ 10.63 (s, 1H), 8.51 (d, *J* = 8.4 Hz, 2H), 7.85 (s, 1H), 7.83–7.71 (m, 5H), 7.50 (m, 2H), 7.41 (m, 1H), 7.22 (td, *J* = 7.6, 0.8 Hz, 1H), 7.00 (td, *J* = 7.6, 0.8 Hz, 1H), 6.84 (d, *J* = 7.6 Hz, 1H). ^{13}C NMR (101 MHz, DMSO) δ 167.66, 142.17, 141.25, 139.74, 136.65, 133.69, 133.17, 129.51, 129.45, 128.49, 127.22, 126.80, 125.47, 121.54, 120.28, 109.84. HRMS (Q-TOF): calculated for $C_{21}H_{15}NO$ 297.1154 $[M + H]^+$, found 298,1233. Purity ≥ 95.0%.

*4.2.20. 3-(3,5-Dibromo-4-hydroxybenzylidene)indolin-2-one (**C13**)*

^{1}H NMR (400 MHz, DMSO) δ 10.33 (m, 1H), 8.74 (s, 8/5H), 7.81 (s, 2/5H), 7.75 (m, 1/5H), 7.52 (d, *J* = 7.6 Hz, 4/5H), 7.44 (s, 4/5H), 7.34 (s, 1/5H), 7.13 (t, *J* = 7.6 Hz, 1/5H), 7.03 (t, *J* = 7.6 Hz, 4/5H), 6.95–6.83 (m, 6/5H), 6.77 (d, *J* = 7.6 Hz, 4/5H). ^{13}C NMR (101 MHz, DMSO) δ 167.75, 152.98, 141.11, 136.54, 134.39, 129.39, 129.10, 126.52, 125.34, 121.66, 121.61, 120.10, 111.55, 109.91. HRMS (Q-TOF): calculated for $C_{15}H_9Br_2NO_2$ 392.9000 $[M + Na]^+$, found 415.8901. Purity ≥ 95.0%.

*4.2.21. 3-((1-Methyl-1H-indol-3-yl)methylene)indolin-2-one (**C15**)*

^{1}H NMR (400 MHz, DMSO) δ 10.51 (s, 1H), 9.40 (s, 1H), 8.22–8.17 (m, 1H), 8.12 (s, 1H), 7.88 (d, *J* = 7.6 Hz, 1H), 7.61–7.55 (m, 1H), 7.36–7.25 (m, 2H), 7.14 (td, *J* = 7.6, 1.2 Hz, 1H), 6.99 (td, *J* = 7.6, 0.8 Hz, 1H), 6.85 (d, *J* = 7.6 Hz, 1H), 3.94 (s, 3H). ^{13}C NMR (101 MHz, DMSO) δ 168.54, 139.67, 137.41, 137.01, 129.17, 127.24, 127.01, 126.13, 123.08, 121.52, 121.00, 119.47, 119.19, 119.05, 111.15, 110.89, 109.45, 33.89. HRMS (Q-TOF): calculated for $C_{18}H_{14}N_2O$ 274.1106$[M + H]^+$, found 275.1180. Purity ≥ 95.0%.

*4.2.22. 3-((5-Methylpyrazin-2-yl)methylene)indolin-2-one (**C17**)*

^{1}H NMR (400 MHz, DMSO) δ 10.64 (s, 1H), 8.96 (d, *J* = 0.8 Hz, 1H), 8.87 (d, *J* = 7.6 Hz, 1H), 8.83 (s, 1H), 7.60 (s, 1H), 7.30 (td, *J* = 7.6, 0.8 Hz, 1H), 6.99 (td, *J* = 7.6, 0.8 Hz, 1H), 6.88 (d, *J* = 7.6 Hz, 1H), 2.59 (s, 3H). ^{13}C NMR (101 MHz, DMSO) δ 169.39, 154.26, 148.10, 146.60, 144.56, 144.19, 131.61, 130.87, 130.35, 128.23, 121.77, 110.22, 21.87. HRMS (Q-TOF): calculated for $C_{14}H_{11}N_3O$ 237.0902 $[M + H]^+$, found 238.0980. Purity ≥ 95.0%.

*4.2.23. 3-((2-Chloro-6-methoxyquinolin-3-yl)methylene)indolin-2-one (**C18**)*

^{1}H NMR (400 MHz, DMSO) δ 10.74 (s, 3/10*H*), 10.23 (s, 7/10*H*), 8.71 (s, 3/10*H*), 8.44 (s, 7/10*H*), 7.95 (d, *J* = 10.0 Hz, 3/10*H*), 7.87 (d, *J* = 9.2 Hz, 7/10*H*), 7.62 (s, 3/10*H*), 7.56–7.52 (m, 6/10*H*), 7.48 (d, *J* = 2.4 Hz, 7/10*H*), 7.44 (dd, *J* = 9.2, 2.8 Hz, 7/10*H*), 7.37 (d, *J* = 7.2 Hz, 7/10*H*), 7.23 (m, 1H), 7.14 (d, *J* = 7.6 Hz, 3/10*H*), 7.00 (m, 7/10*H*), 6.91 (d, *J* = 7.6 Hz, 3/10*H*), 6.81 (m, 1H), 5.95 (d, *J* = 4.4 Hz, 7/10*H*), 3.91 (s, 21/10*H*), 3.80 (s, 9/10*H*). ^{13}C NMR (101 MHz, DMSO) δ 168.42, 158.64, 146.35, 143.84, 143.41, 138.39, 131.40, 130.76, 130.34, 129.71, 128.25, 127.83, 124.52, 123.14, 122.03, 120.80, 110.87, 106.84, 56.25. HRMS (Q-TOF): calculated for $C_{19}H_{13}ClN_2O_2$ 336.0666 $[M + Na]^+$, found 359.0561 Purity ≥ 95.0%.

*4.2.24. 3-((5-Bromofuran-2-yl)methylene)indolin-2-one (**C19**)*

^{1}H NMR (400 MHz, DMSO) δ 10.60 (s, 1H), 8.21 (d, *J* = 8.0 Hz, 1H), 7.29 m, 2H), 7.04 (t, *J* = 7.6 Hz, 1H), 6.96 (d, *J* = 3.6 Hz, 1H), 6.89 (d, *J* = 7.6 Hz, 1H). ^{13}C NMR (101 MHz, DMSO) δ 169.53, 153.09, 143.30, 130.49, 126.94, 124.69, 123.23, 123.03, 121.85, 121.50, 118.61, 116.17, 110.40. HRMS (Q-TOF): calculated for $C_{13}H_8BrNO_2$ 288.9738 $[M + H]^+$, found 289.9805. Purity ≥ 95.0%.

*4.2.25. 3-(4-Hydroxybenzylidene)-5-nitroindolin-2-one (**D1**)*

^{1}H NMR (400 MHz, DMSO) δ 11.25 (s, 1H), 10.41 (s, 4/5H), 10.33 (s, 1/5H), 8.65 (d, *J* = 2.0 Hz, 4/5H), 8.50 (m, 2H), 8.20–8.08 (m, 9/5H), 7.76 (s, 1/5H), 7.70 (d, *J* = 8.4 Hz, 1/5H), 7.05 (d, *J* = 8.8 Hz, 1/5H), 6.99 (d, *J* = 8.4 Hz, 4/5H), 6.96 (d, *J* = 8.8 Hz, 2/5H), 6.89 (d, *J* = 8.8 Hz, 8/5/H). ^{13}C NMR (101 MHz, DMSO) δ 169.70, 168.13, 161.61, 160.65, 148.52, 145.81, 142.39, 141.94, 141.85, 140.65, 136.15, 132.80, 126.88, 126.24, 125.83. HRMS (Q-TOF): calculated for $C_{15}H_{10}N_2O_4$ 282.0641 $[M + Na]^+$, found 305.0541. Purity ≥ 95.0%.

*4.2.26. 3-(4-Methylbenzylidene)-5-nitroindolin-2-one (**D2**)*

^{1}H NMR (400 MHz, DMSO) δ 11.31 (m, 1H), 8.69 (d, *J* = 2.0 Hz, 3/4H), 8.43 (d, *J* = 2.4 Hz, 1/4H), 8.39 (d, *J* = 8.0 Hz, 6/4H), 8.17 (m, 7/4H), 7.81 (s, 1/4H), 7.69 (d, *J* = 8.0 Hz, 1/2H), 7.40 (d, *J* = 8.0 Hz, 1/2H), 7.33 (d, *J* = 8.0 Hz, 3/2H), 7.06 (d, *J* = 8.6 Hz, 1/4H), 7.01 (d, *J* = 8.6 Hz, 3/4H), 2.43 (s, 3/4H), 2.39 (s, 9/4H). ^{13}C NMR (101 MHz, DMSO) δ 169.38, 148.89, 141.97, 141.32, 139.97, 131.27, 130.19, 129.98, 126.76, 125.44, 121.76, 117.74, 110.47, 21.64. HRMS (Q-TOF): calculated for $C_{16}H_{12}N_2O_3$ 280.0848 $[M + Na]^+$, found 303.0741. Purity ≥ 95.0%.

*4.2.27. 5-Nitro-3-(pyridin-2-ylmethylene)indolin-2-one (**D3**)*

^{1}H NMR (400 MHz, DMSO) δ 11.33 (s, 1H), 10.11 (d, *J* = 2.4 Hz, 1H), 8.92 (d, *J* = 4.4 Hz, 1H), 8.25 (dd, *J* = 8.6, 2.4 Hz, 1H), 8.02 (m, 2H), 7.75 (s, 1H), 7.62–7.49 (m, 1H), 7.06 (d, *J* = 8.6 Hz, 1H). ^{13}C NMR (101 MHz, DMSO) δ 170.01, 153.00, 150.12, 149.66, 142.34, 138.11, 137.13, 130.00, 127.85, 127.55, 125.52, 124.14, 122.23, 110.15. HRMS (Q-TOF): calculated for $C_{14}H_9N_3O_3$ 267.0644 $[M + H]^+$, found 268.0715. Purity ≥ 95.0%.

*4.2.28. 3-(3-Hydroxy-4-methoxybenzylidene)-5-nitroindolin-2-one (**D5**)*

^{1}H NMR (400 MHz, DMSO) δ 11.16 (s, 1H), 9.28 (s, 1H), 8.66 (d, *J* = 2.4 Hz, 1/2H), 8.56 (d, *J* = 2.0 Hz, 1/2H), 8.27 (d, *J* = 2.0 Hz, 1/2H), 8.15 (m,1H), 8.07 (s, 1/2H), 7.94 (dd, *J* = 8.4, 2.0 Hz, 1/2H), 7.71 (s, 1/2H), 7.29–7.23 (m, 1H), 7.15–6.97 (m, 2H), 3.89 (d, *J* = 2.0 Hz, 3H). ^{13}C NMR (101 MHz, DMSO) δ 169.64, 168.00, 151.71, 150.67, 148.66, 147.20, 146.30, 145.96, 142.43, 142.00, 141.96, 140.51, 127.56, 127.46, 126.77, 126.61, 126.38, 124.84, 123.78, 123.12, 122.00, 121.76, 119.72, 117.72, 116.85, 115.43, 112.59, 111.85, 110.35, 109.51, 56.21, 56.13. Purity ≥ 95.0%.

*4.2.29. 3-([1,1′-Biphenyl]-4-ylmethylene)-5-nitroindolin-2-one (**D12**)*

^{1}H NMR (400 MHz, DMSO) δ 11.36 (s, 1H), 8.73 (d, *J* = 2.0 Hz, 1/2H), 8.58 (d, *J* = 8.2 Hz, 1/2H), 8.46 (d, *J* = 2.0 Hz, 1/2H), 8.28 (s, 1H), 8.19 (td, *J* = 8.4, 2.4 Hz, 1H), 7.94–7.77 (m, 11/2H), 7.52 (dd, *J* = 13.2, 7.2 Hz, 2H), 7.43 (dd, *J* = 13.2, 7.2 Hz, 1H), 7.08 (d, *J* = 8.6 Hz, 1/2H), 7.03 (d, *J* = 8.6 Hz, 1/2H). ^{13}C NMR (101 MHz, DMSO) δ 169.33, 167.87, 149.03, 146.56, 143.10, 142.57, 142.05, 140.67, 139.57, 139.45, 133.73, 133.28, 133.25, 130.88, 129.60, 129.54, 128.69, 127.48, 127.31, 127.28, 126.95, 126.24, 126.18, 125.71, 124.89,

121.72, 117.96, 116.11, 110.60, 109.83. HRMS (Q-TOF): calculated for $C_{21}H_{14}N_2O_3$ 342.1004 $[M + Na]^+$, found 365.0903. Purity ≥ 95.0%.

4.2.30. 3-(3,5-Dibromo-4-hydroxybenzylidene)-5-nitroindolin-2-one (D13)

^{1}H NMR (400 MHz, DMSO) δ 11.30 (m, 1H), 8.84 (s, 8/5H), 8.61 (d, *J* = 2.0 Hz, 4/5H), 8.42 (d, *J* = 2.0 Hz, 1/5H), 8.19 (dd, *J* = 8.6, 2.4 Hz, 1/5H), 8.13 (dd, *J* = 8.6, 2.4 Hz, 4/5H), 8.05 (s, 4/5H), 8.01 (s, 2/5H), 7.69 (s, 1/5H), 7.06 (d, *J* = 8.6 Hz, 1/5H), 7.00 (d, *J* = 8.6 Hz, 4/5H). ^{13}C NMR (101 MHz, DMSO) δ 168.02, 145.99, 142.43, 138.59, 137.43, 134.23, 126.51, 124.92, 115.36, 112.67, 112.21, 109.66. HRMS (Q-TOF): calculated for $C_{15}H_8Br_2N_2O_4$ 439.8830 $[M + Na]^+$, found 462.8714. Purity ≥ 95.0%.

4.2.31. 3-(2-Chloro-4-hydroxybenzylidene)-5-nitroindolin-2-one (D14)

^{1}H NMR (400 MHz, DMSO) δ 11.30 (s, 1H), 8.57 (d, *J* = 2.4 Hz, 1/5H), 8.49 (d, *J* = 8.8 Hz, 1/5H), 8.27–8.10 (m, 2H), 7.81–7.72 (m, 8/5H), 7.10–7.04 (m, 4/5H), 7.00 (d, *J* = 8.8 Hz, 1/5H), 6.94 (m, 4/5H), 6.79 (dd, *J* = 8.8, 2.0 Hz, 1/5H). ^{13}C NMR (101 MHz, DMSO) δ 169.17, 161.24, 148.89, 142.04, 135.79, 135.53, 132.26, 126.87, 125.82, 122.60, 121.60, 117.87, 117.23, 115.25, 110.56. HRMS (Q-TOF): calculated for $C_{15}H_9ClN_2O_4$ 316.0251 $[M + Na]^+$, found 339.0143. Purity ≥ 95.0%.

4.2.32. 3-((1-Methyl-1H-indol-3-yl)methylene)-5-nitroindolin-2-one (D15)

^{1}H NMR (400 MHz, DMSO) δ 11.23 (s, 1H), 9.48 (s, 1H), 8.95 (d, *J* = 2.0 Hz, 1H), 8.54 (s, 1H), 8.41 (m, 1H), 8.09 (dd, *J* = 8.8, 2.4 Hz, 1H), 7.61 (m, 1H), 7.41–7.27 (m, 2H), 7.02 (d, *J* = 8.4 Hz, 1H), 3.97 (s, 3H). ^{13}C NMR (101 MHz, DMSO) δ 169.47, 149.91, 146.94, 143.10, 136.94, 130.05, 127.36, 125.77, 122.82, 122.67, 121.67, 121.47, 116.70, 112.56, 110.45, 56.11. HRMS (Q-TOF): calculated for $C_{18}H_{13}N_3O_3$ 319.0957 $[M + Na]^+$, found 342.0851. Purity ≥ 95.0%.

4.2.33. 3-((5-(2-Fluorophenyl)-1H-pyrrol-3-yl)methylene)-5-nitroindolin-2-one (D16)

^{1}H NMR (400 MHz, DMSO) δ 12.27 (s, 1/5H), 12.11 (s, 4/5H), 11.15 (d, *J* = 12.9 Hz, 1H), 8.85 (d, *J* = 2.4 Hz, 1/5H), 8.54 (d, *J* = 2.0 Hz, 4/5H), 8.32 (s, 4/5H), 8.21–8.15 (m, 1H), 8.09 (dd, *J* = 8.4, 2.0 Hz, 4/5H), 7.78 (m, 7/5H), 7.61 (s, 4/5H), 7.39–7.26 (m, 3H), 7.21 (s, 1/5H), 7.03 (m, 1H). ^{13}C NMR (101 MHz, DMSO) δ 168.37, 145.26, 142.19, 135.31, 130.52, 128.63 (d, *J* = 8.1 Hz), 127.23, 127.05 (d, *J* = 3.0 Hz), 126.90, 125.31, 125.28, 123.72, 121.46, 120.18, 117.48, 116.90, 116.68, 114.28, 114.11 (d, *J* = 9.1 Hz), 109.30. HRMS (Q-TOF): calculated for $C_{19}H_{12}FN_3O_3$ 349.0863 $[M + Na]^+$, found 372.0758. Purity ≥ 95.0%.

4.2.34. 3-(3,5-Dibromo-4-methoxybenzylidene)-5-nitroindolin-2-one (D13a)

^{1}H NMR (400 MHz, DMSO) δ 11.41 (s, 1H), 8.82 (s, 2H), 8.65 (d, *J* = 2.4 Hz, 1H), 8.19 (dd, *J* = 8.6, 2.4 Hz, 1H), 8.16 (s, 1H), 7.03 (d, *J* = 8.6 Hz, 1H), 3.88 (s, 2H).

^{13}C NMR (101 MHz, DMSO) δ 167.73, 155.65, 146.85, 142.62, 136.93, 134.16, 133.07, 126.44, 126.22, 125.69, 118.46, 117.66, 110.10, 61.15. HRMS (Q-TOF): calculated for $C_{16}H_{10}Br_2N_2O_4$ 453.8987 $[M + Na]^+$, found 476.3730. Purity ≥ 95.0%.

4.2.35. 3-(2-Chloro-4-hydroxybenzylidene)-1-methylindolin-2-one (E14)

^{1}H NMR (400 MHz, DMSO) δ 8.91 (d, *J* = 1.6 Hz, 3/10*H*), 8.10 (m, 3/10*H*), 7.75–7.64 (m, 2H), 7.61–7.54 (m, 7/5H), 7.27 (m, 1H), 6.99 (m, 27/10*H*), 6.88 (d, *J* = 8.4 Hz, 3/10*H*), 3.21 (d, *J* = 8.4 Hz, 3H). ^{13}C NMR (101 MHz, DMSO) δ 168.06, 158.08, 144.05, 136.68, 134.60, 132.19, 130.72, 129.82, 125.10, 123.87, 122.06, 121.10, 118.91, 117.74, 109.21, 26.43. HRMS (Q-TOF): calculated for $C_{16}H_{12}ClNO2$ 285.0557 $[M + Na]^+$, found 308.0449. Purity ≥ 95.0%.

4.3. Protein purification

HsClpP was expressed and purified as described previously. Wildtype HsClpP (without mitochondrial targeting sequences) were expressed in E. coli. To induce protein expression, bacteria, after reaching OD600 0.6 ~ 0.8, were treated with 1 mM isopropyl-1-thio-B-D-galactopyranoside for 4 h at 37 °C, harvested by centrifugation, and disrupted in lysis buffer (25 mM Tris-HCl (pH 7.5), 0.5 M NaCl). Following cell lysis, the insoluble material was removed by centrifugation ($1.4x10^4$ rpm for 30 min) and the supernatant was passed through a 5 mL Ni-sepharose high-performance (GE) column pre-equilibrated with lysis buffer. The protein was eluted with 400 mM imidazole, diluted with 25 mL of dialysis buffer (25 mM Tris-HCl (pH 7.5), 0.1 M NaCl), and dialyzed overnight at 4 °C with light stirring into 4 L of dialysis buffer. The dialyzed material was then passed through a second 5 mL Ni-column and the flow-through solution containing untagged HsClpP was collected. All fractions were analyzed by SDS-PAGE.

4.4. HsClpP enzymatic assays

Assay buffer consisted of 25 mM Tris-HCl, pH 7.5, 0.1 M NaCl pH 8 for AC-WLA-AMC assay. 1.0 μM HsClpP was dissolved in the assay buffer, incubated at 37C for 10 min, and mixed with increasing concentrations of synthesized compounds in 96 well plates at 80 μL per well in triplicate. Fluorescent tagged- substrates, AC-WLA-AMC (100 μM), were then added to each well and fluorescence was measured at 380/460 nm every 5 min for 90 min at 37 °C. Experiments were performed three times with triplicate wells in each experiment.

For the protease activity assay, the buffer solution consisted of 25 mM Hepes, pH 7.5, 20 mM MgCl2, 30 mM KCl, 0.03% Tween 20, 10% glycerol, and 2 mM DTT. Each reaction contained 1 μM HsClpP, 1 μM ONC201, and an ATP-regenerating system (4 mM ATP, 20 U/mL creatine kinase, and 16 mM creatine phosphate). 4 μM FITC-casein was then added to each well, and the fluorescence was measured at 485/535 nm for 60 min. Experiments were performed three times with triplicate wells in each experiment.

4.5. In vitro inhibitory activity

Hela, HepG2, HCT116, MCF-7 and SKOV3 cells were seeded in 96-well plates at a density of 5×10^3 cells/well and cultured for 24 h, following the addition of different concentrations of compounds. The cells were further cultured for 72 h, with 0.5% DMSO as the solvent control group. Then cells were incubated for 1–4 h with 5 mg/ml of 3-(4,5-dimethylthiazol-2-yl)-2,5-diphenyltetrazolium bromide (MTT) solution, and the formazan crystals were dissolved with 100 mL of DMSO. After gentle shaking for 10 min, the optical density (OD) was measured at 570 nm using a Spectra MAX M5 microplate spectrophotometer. Each treatment was performed in triplicate. Results were analyzed with GraphPad Prism 6 and data were shown as Mean ± SD.

4.6. Molecular docking

Molecular docking studies were carried out using the Schrodinger software. The protein was constructed based on the X-ray structure of HsClpP, which was available through the RCSB Protein Data Bank (PDB code: 1TG6). Both the compounds and the structure of HsClpP were prepared and optimized using Schrodinger. The protein was prepared with adding hydrogens, deleting water molecules. Compound I was docked into the catalytic site using the Glide XP docking procedure.

4.7. Wound healing assay

Hela cells were seed in 6 well plates and cultured until confluent. Using a pipette tip makes a straight scratch to simulate a wound, 24 h after treatment by compound I at 5 μM. Cells were washed twice to

remove detached cells and debris. Then, size of wounds were observed and measured at the indicated times.

4.8. Western blot analysis

Total cellular proteins were extracted in RIPA buffer (Beyotime Biotechnology) supplemented with protease inhibitor PMSF (Sigma-Aldrich). Protein concentrations were determined with BCA protein assay kit (Beyotime Biotechnology). Equal amounts of protein were run out on 10% SDS-PAGE gel and subsequently transferred onto PVDF membranes (Millipore). Membranes were blocked in 5% skimmed milk and incubated with the following primary antibodies at 4 °C overnight. Second antibodies were used at a dilution of 1:2000. Enhanced chemiluminescence (ECL) and digital imaging (Clinx Science Instruments, Chemiscope 5300) were used for detection of target proteins.

4.9. Detection of ROS

The ROS level was detected using dihydroethidium (DHE, Beyotime Biotechnology), which measures the cellular superoxide. Briefly, after treatment with compound I for 72 h, cells were harvested and stained with 10 μM DHE dissolved in pre-warmed PBS for 15 min in the dark. The fluorescence intensity of DHE was measured according to the manufacturer's instructions.

Declaration of Competing Interest

The authors declare that they have no known competing financial interests or personal relationships that could have appeared to influence the work reported in this paper.

Acknowledgements

This work was financially supported by grants from National Natural Science Foundation of China (Grant NO. 81973368) and National Megaproject for Innovative Drugs (2019ZX09721001-001-001).

Appendix A. Supplementary material

Supplementary data to this article can be found online at https://doi.org/10.1016/j.bioorg.2021.104820.

References

[1] A. Carvalho, M. Rodríguez, R. Matthiesen, Review and literature mining on proteostasis factors and cancer, Methods Mol. Biol. (Clifton, N.J.) 1449 (2016) 71–84. https://doi.org/10.1007/978-1-4939-3756-1_2.

[2] E. Leung, A. Datti, M. Cossette, J. Goodreid, S. McCaw, M. Mah, A. Nakhamchik, K. Ogata, M. El Bakkouri, Y. Cheng, S. Wodak, B. Eger, E. Pai, J. Liu, S. Gray-Owen, R. Batey, W. Houry, Activators of cylindrical proteases as antimicrobials: identification and development of small molecule activators of ClpP protease, Chem. Biol. 18 (9) (2011) 1167–1178, https://doi.org/10.1016/j.chembiol.2011.07.023.

[3] Q. Zhao, J. Wang, I.V. Levichkin, S. Stasinopoulos, M.T. Ryan, N.J. Hoogenraad, A mitochondrial specific stress response in mammalian cells, The EMBO J. 21 (17) (2002) 4411–4419, https://doi.org/10.1093/emboj/cdf445.

[4] A. Cole, Z. Wang, E. Coyaud, V. Voisin, M. Gronda, Y. Jitkova, R. Mattson, R. Hurren, S. Babovic, N. Maclean, I. Restall, X. Wang, D.V. Jeyaraju, M.A. Sukhai, S. Prabha, S. Bashir, A. Ramakrishnan, E. Leung, Y.H. Qia, N. Zhang, K.R. Combes, T. Ketela, F. Lin, W.A. Houry, A. Aman, R. Al-Awar, W. Zheng, E. Wienholds, C. J. Xu, J. Dick, J.C. Wang, J. Moffat, M.D. Minden, C.J. Eaves, G.D. Bader, Z. Hao, S. M. Kornblau, B. Raught, A.D. Schimmer, Inhibition of the mitochondrial protease ClpP as a therapeutic strategy for human acute myeloid leukemia, Cancer Cell 27 (6) (2015) 864–876, https://doi.org/10.1016/j.ccell.2015.05.004.

[5] J. Ishizawa, S.F. Zarabi, R.E. Davis, O. Halgas, T. Nii, Y. Jitkova, R. Zhao, J. St-Germain, L.E. Heese, G. Egan, V.R. Ruvolo, S.H. Barghout, Y. Nishida, R. Hurren, W. Ma, M. Gronda, T. Link, K. Wong, M. Mabanglo, K. Kojima, G. Borthakur, N. MacLean, M.C.J. Ma, A.B. Leber, M.D. Minden, W. Houry, H. Kantarjian, M. Stogniew, B. Raught, E.F. Pai, A.D. Schimmer, M. Andreeff, Mitochondrial ClpP-mediated proteolysis induces selective cancer cell lethality, Cancer Cell 35 (5) (2019) 721–737.e9, https://doi.org/10.1016/j.ccell.2019.03.014.

[6] J.H. Seo, D.B. Rivadeneira, M.C. Caino, Y.C. Chae, D.W. Speicher, H.Y. Tang, V. Vaira, S. Bosari, A. Palleschi, P. Rampini, A.V. Kossenkov, L.R. Languino, D.C. Altieri, The Mitochondrial unfoldase-peptidase complex ClpXP controls bioenergetics stress and metastasis, PLoS Biol. 14(7) (2016) e1002507. https://doi.org/10.1371/journal.pbio.1002507.

[7] K. Wong, M. Mabanglo, T. Seraphim, A. Mollica, Y. Mao, K. Rizzolo, E. Leung, M. Moutaoufik, L. Hoell, S. Phanse, J. Goodreid, L. Barbosa, C. Ramos, M. Babu, V. Mennella, R. Batey, A. Schimmer, W. Houry, Acyldepsipeptide analogs dysregulate human mitochondrial ClpP protease activity and cause apoptotic cell death, Cell Chem. Biol. 25 (8) (2018) 1017–1030.e9, https://doi.org/10.1016/j.chembiol.2018.05.014.

[8] A. Cormio, C. Musicco, G. Gasparre, G. Cormio, V. Pesce, A.M. Sardanelli, M. N. Gadaleta, Increase in proteins involved in mitochondrial fission, mitophagy, proteolysis and antioxidant response in type I endometrial cancer as an adaptive response to respiratory complex I deficiency, Biochem. Biophys. Res. Commun. 491 (1) (2017) 85–90, https://doi.org/10.1016/j.bbrc.2017.07.047.

[9] V. Bhandari, K.S. Wong, J.L. Zhou, M.F. Mabanglo, R.A. Batey, W.A. Houry, The role of ClpP protease in bacterial pathogenesis and human diseases, ACS Chem. Biol. 13 (6) (2018) 1413–1425, https://doi.org/10.1021/acschembio.8b00124.

[10] E. Zeiler, V.S. Korotkov, K. Lorenz-Baath, T. Böttcher, S.A. Sieber, Development and characterization of improved β-lactone-based anti-virulence drugs targeting ClpP, Bioorg. Med. Chem. 20 (2) (2012) 583–591, https://doi.org/10.1016/j.bmc.2011.07.047.

[11] T.F. Gronauer, M.M. Mandl, M. Lakemeyer, M.W. Hackl, M. Meßner, V.S. Korotkov, J. Pachmayr, S.A. Sieber, Design and synthesis of tailored human caseinolytic protease P inhibitors, Chem. Commun. (Camb.) 54 (70) (2018) 9833–9836, https://doi.org/10.1039/c8cc05265d.

[12] M.W. Hackl, M. Lakemeyer, M. Dahmen, M. Glaser, A. Pahl, K. Lorenz-Baath, T. Menzel, S. Sievers, T. Böttcher, I. Antes, H. Waldmann, S.A. Sieber, Phenyl esters are potent inhibitors of caseinolytic protease P and reveal a stereogenic switch for deoligomerization, J. Am. Chem. Soc. 137 (26) (2015) 8475–8483, https://doi.org/10.1021/jacs.5b03084.

[13] J. Tan, J.J. Grouleff, Y. Jitkova, D.B. Diaz, E.C. Griffith, W. Shao, A.F. Bogdanchikova, G. Poda, A.D. Schimmer, R.E. Lee, A.K. Yudin, De Novo design of boron-based peptidomimetics as potent inhibitors of human ClpP in the presence of human ClpX, J. Med. Chem. 62(13) (2019) 6377–6390. https://doi.org/10.1021/acs.jmedchem.9b00878.

[14] K. Knott, J. Fishovitz, S. Thorpe, I. Lee, W. Santos, N-terminal peptidic boronic acids selectively inhibit human ClpXP, Org. Biomol. Chem. 8 (15) (2010) 3451–3456, https://doi.org/10.1039/c004247a.

[15] P.R. Graves, L.J. Aponte-Collazo, E.M.J. Fennell, A.C. Graves, A.E. Hale, N. Dicheva, L.E. Herring, T.S.K. Gilbert, M.P. East, I.M. McDonald, M.R. Lockett, H. Ashamalla, N.J. Moorman, D.S. Karanewsky, E.J. Iwanowicz, E. Holmuhamedov, L.M. Graves, Mitochondrial protease ClpP is a target for the anticancer compounds ONC201 and related analogues, ACS Chem. Biol. 14 (5) (2019) 1020–1029, https://doi.org/10.1021/acschembio.9b00222.

[16] M. Stahl, V.S. Korotkov, D. Balogh, L.M. Kick, M. Gersch, A. Pahl, P. Kielkowski, K. Richter, S. Schneider, S.A. Sieber, Selective activation of human caseinolytic protease P (ClpP), Angew. Chem. Int. Ed. Engl. 57 (44) (2018) 14602–14607, https://doi.org/10.1002/anie.201808189.